

Seismic responses in fractured reservoir rocks with induced attenuation

---Estimation of fracture weaknesses and integrated attenuation factors

Huaizhen Chen* and Kris Innanen

CREWES annual meeting 2017

Outline

- Introduction
- Stiffness parameters of fractured and attenuative rocks
- Linearized reflection coefficient and seismic amplitude difference inversion
- Examples
- Discussions and conclusions

Introduction

- Expression of the normal fracture weakness for fluid saturated fractured rocks (Bakulin et al., 2000)

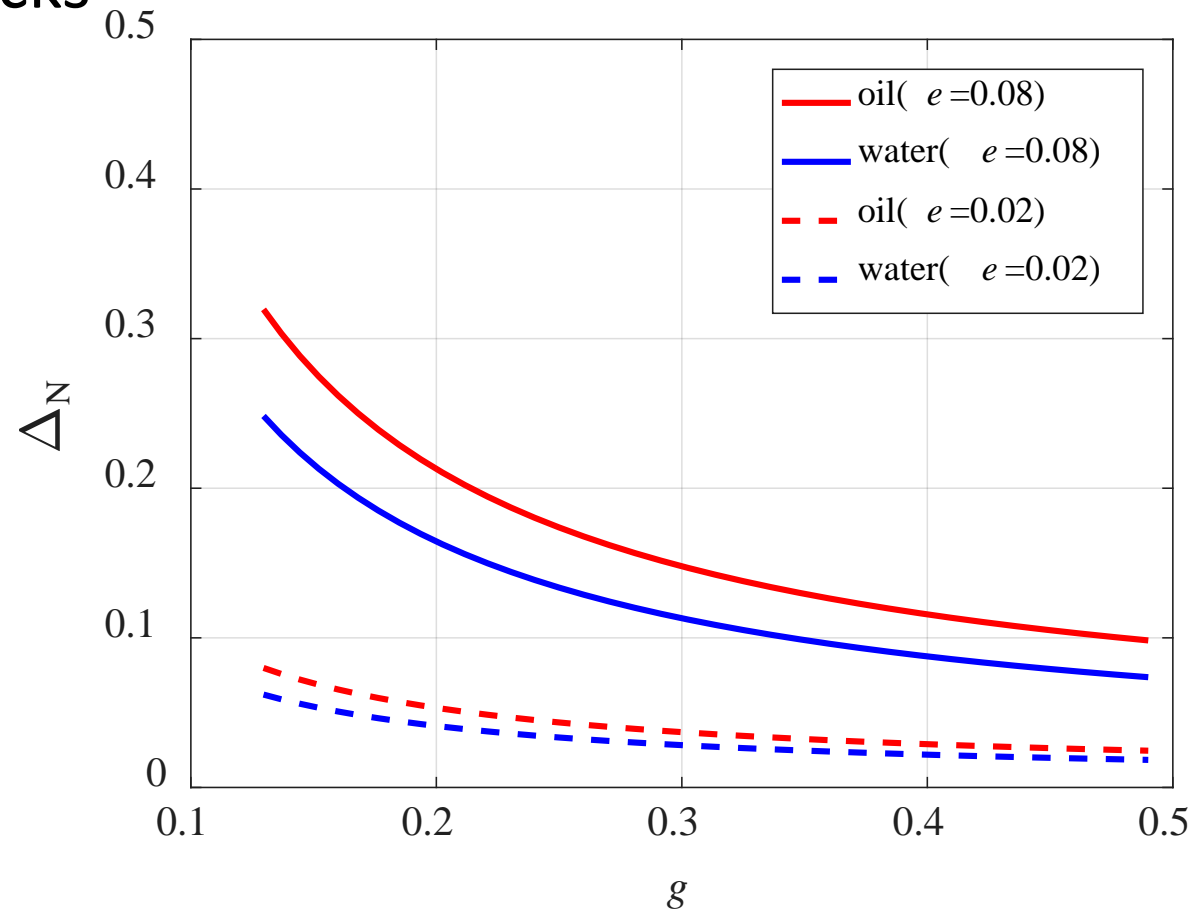
$$\Delta_N = \frac{4e}{3g(1-g) \left[1 + \frac{1}{\pi(1-g)} \left(\frac{k_f + 4/3\mu_f}{\mu\alpha} \right) \right]}$$

- where e is fracture density, k_f and μ_f are effective moduli of mixture of water and oil, α is fracture aspect ratio, g and μ are elastic parameters of isotropic and elastic background.

	K_f (GPa)	μ_f (GPa)
Water	2.15	0
Oil	1.5	0

Introduction

- Variations of the normal fracture weakness for oil- and water saturated rocks



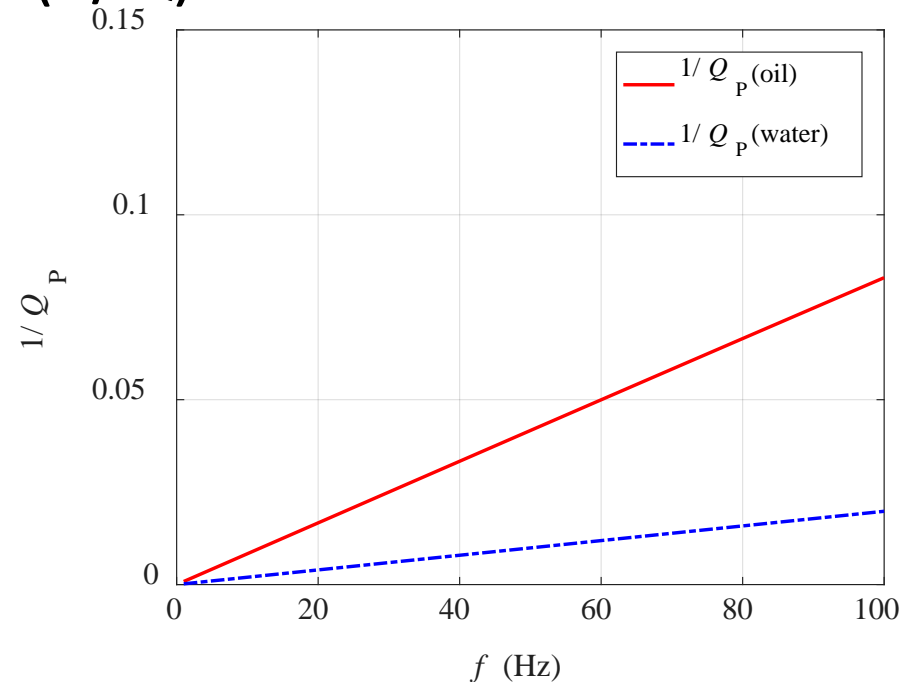
The normal fracture weakness is not sensitive to distinguish oil and water reservoirs.

Introduction

- Incorporating fluid viscosity influences

	η_f (cp)
Water	1
Oil	8

- Attenuation factor ($1/Q$) variations



Results obtained using the extended squirt model (Dvorkin et al, 1996).

Stiffness parameters of fractured and attenuative rocks

- Elastic and anisotropic linear-slip theory for HTI media (Schoenberg and Sayers, 1995)

$$\mathbf{C} = \begin{bmatrix} M(1-\Delta_N) & \lambda(1-\Delta_N) & \lambda(1-\Delta_N) & 0 & 0 & 0 \\ \lambda(1-\Delta_N) & M(1-\chi^2\Delta_N) & \lambda(1-\chi\Delta_N) & 0 & 0 & 0 \\ \lambda(1-\Delta_N) & \lambda(1-\chi\Delta_N) & M(1-\chi^2\Delta_N) & 0 & 0 & 0 \\ 0 & 0 & 0 & \mu & 0 & 0 \\ 0 & 0 & 0 & 0 & \mu(1-\Delta_T) & 0 \\ 0 & 0 & 0 & 0 & 0 & \mu(1-\Delta_T) \end{bmatrix}$$

- Introducing the complex normal and tangential fracture weaknesses (Chichinina et al, 2006)

$$\Delta_N \rightarrow \overline{\Delta_N} = \Delta_N - i \frac{1}{Q_N} \Delta_N,$$

$$\Delta_T \rightarrow \overline{\Delta_T} = \Delta_T - i \frac{1}{Q_T} \Delta_T,$$

Induced attenuation factors

Stiffness parameters of fractured and attenuative rocks

- Relating complex fracture weaknesses to fracture properties (fracture density) and fluid parameters (fluid moduli and viscosity)

$$\overline{\Delta}_N = \frac{M}{\mu} \overline{U}_{33} e, \quad \overline{\Delta}_T = \overline{U}_{11} e$$

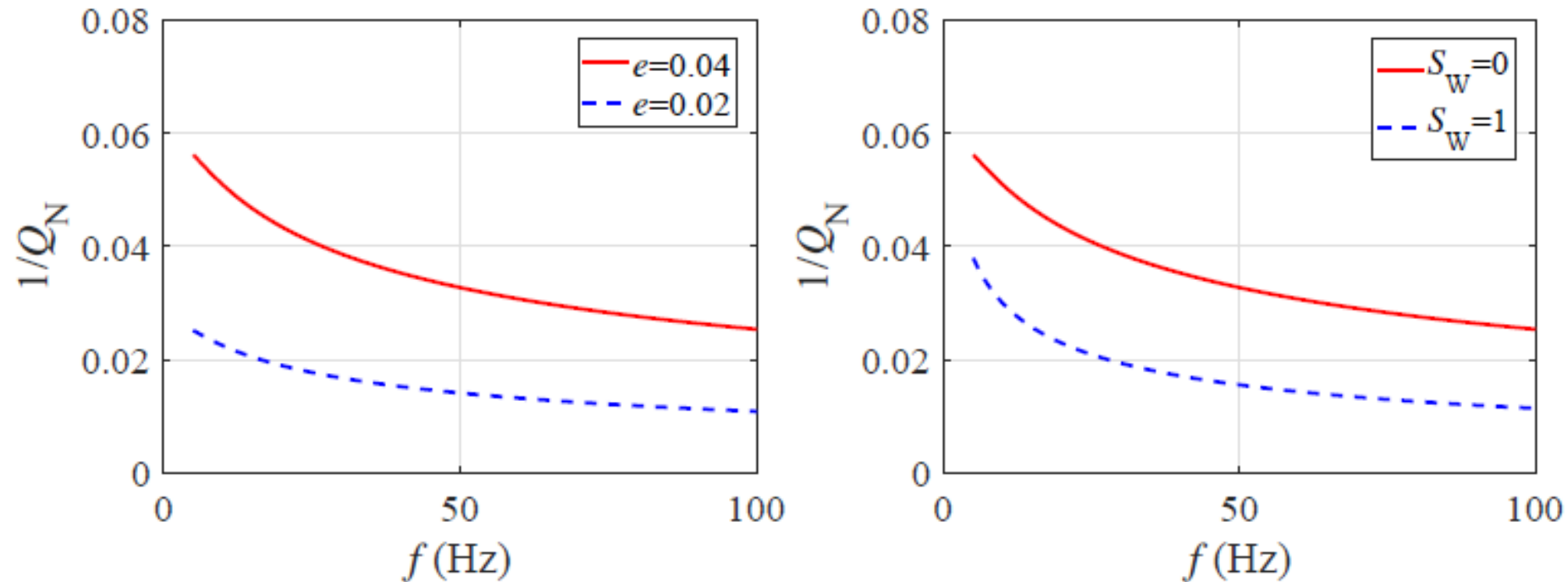
• where

$$\overline{U}_{11} = \frac{16}{3} \frac{M}{3\lambda + 4\mu} \frac{1}{1 + \overline{\Gamma}(\omega)} \quad \text{and} \quad \overline{\Gamma}(\omega) = \frac{4a}{\pi c} \left(\frac{i\omega\eta_f}{\mu} \right) \left(\frac{M}{3\lambda + 4\mu} \right)$$

$$\overline{U}_{33} = \frac{4}{3} \frac{M}{\lambda + \mu} \frac{1}{1 + \overline{\Psi}(\omega)} \quad \overline{\Psi}(\omega) = \frac{a}{\pi c} \frac{K_f}{\mu} \frac{M}{\lambda + \mu} \left[1 - \frac{3(1-i)}{2c} \sqrt{\frac{\phi K_f P_m}{2\omega\eta_f}} \right]^{-1}$$

- In the seismic frequency range (1-100Hz), $\overline{\Gamma}(\omega)$ is approximately equal to zero (Pointer et al., 2000), which indicates the tangential fracture weakness is real and $1/Q_T$ is zero.

Stiffness parameters of fractured and attenuative rocks



Induced attenuation factor increases with fracture density.

Oil saturated rocks exhibit higher induced attenuation than water saturated rocks.

Stiffness parameters of fractured and attenuative rocks

- Combining the intrinsic and induced attenuations

$$\bar{\mathbf{C}} = \begin{bmatrix} \bar{M}(1-\bar{\Delta}_N) & \bar{\lambda}(1-\bar{\Delta}_N) & \bar{\lambda}(1-\bar{\Delta}_N) & 0 & 0 & 0 \\ \bar{\lambda}(1-\bar{\Delta}_N) & \bar{M}(1-\bar{\chi}^2\bar{\Delta}_N) & \bar{\lambda}(1-\bar{\chi}\bar{\Delta}_N) & 0 & 0 & 0 \\ \bar{\lambda}(1-\bar{\Delta}_N) & \bar{\lambda}(1-\bar{\chi}\bar{\Delta}_N) & \bar{M}(1-\bar{\chi}^2\bar{\Delta}_N) & 0 & 0 & 0 \\ 0 & 0 & 0 & \bar{\mu} & 0 & 0 \\ 0 & 0 & 0 & 0 & \bar{\mu}(1-\Delta_T) & 0 \\ 0 & 0 & 0 & 0 & 0 & \bar{\mu}(1-\Delta_T) \end{bmatrix}$$

- where

$$\bar{M} = \rho \left[\alpha_E \left(1 + \frac{i}{2Q_P} \right) \right]^2 \approx M \left(1 + \frac{i}{Q_P} \right), \quad \bar{\mu} = \rho \left[\beta_E \left(1 + \frac{i}{2Q_S} \right) \right]^2 \approx \mu \left(1 + \frac{i}{Q_S} \right)$$

the intrinsic attenuation

Stiffness parameters of fractured and attenuative rocks

- Real parts of simplified stiffness parameters involving influences of integrated attenuation factors

$$C_{11} \approx M - \frac{M}{Q_{PN}} - M \Delta_N$$

where

$$\frac{1}{Q_{PN}} = \frac{1}{Q_P} \frac{1}{Q_N}$$

$$C_{12} \approx \lambda - \lambda \Delta_N - \frac{M}{Q_{PN}} + \frac{2\mu}{Q_{SN}}$$

$$\frac{1}{Q_{SN}} = \frac{1}{Q_S} \frac{1}{Q_N}$$

$$C_{23} \approx \lambda(1 - \Delta_N) + 2\lambda g \Delta_N - M \frac{1}{Q_{PN}} + 2Mg \frac{1}{Q_{PN}} + 2\mu \frac{1}{Q_{SN}} - 4\mu g \frac{1}{Q_{SN}}$$

integrated
attenuation factors

$$C_{33} = M(1 - \Delta_N) + 4Mg \Delta_N - 4Mg^2 \Delta_N + 4Mg \frac{1}{Q_{PN}} - 4Mg^2 \frac{1}{Q_{PN}}$$

$$C_{44} = \mu$$

$$C_{55} = \mu - \mu \Delta_T$$

Linearized reflection coefficient

- Linearized R_{PP} for weakly anisotropic media (Shaw and Sen, 2004)

$$R_{PP} = \frac{1}{4\rho \cos^2 \theta} S$$

- S is the scattering function, ρ is density, and θ is the angle of incidence.

$$S = \Delta\rho\xi + \Delta C_{II}\eta$$

- Linearized reflection coefficient

$$R_{PP}(\theta, \phi) = R_{PP}^{\text{iso-elastic}}(\theta) + R_{PP}^{\text{ani-visco}}(\theta, \phi)$$

$$R_{PP}^{\text{iso-elastic}}(\theta) = \frac{1}{4} \sec^2 \theta \frac{\Delta M}{M} - 2g \sin^2 \theta \frac{\Delta\mu}{\mu} + \frac{\cos 2\theta}{4 \cos^2 \theta} \frac{\Delta\rho}{\rho},$$

$$R_{PP}^{\text{ani-visco}}(\theta, \phi) = P_{Q_{PN}}(\theta, \phi) \Delta \left(\frac{1}{Q_{PN}} \right) + P_{Q_{SN}}(\theta, \phi) \Delta \left(\frac{1}{Q_{SN}} \right) + P_{\Delta_N}(\theta, \phi) \delta_{\Delta_N} + P_{\Delta_T}(\theta, \phi) \delta_{\Delta_T}.$$

Seismic amplitude difference inversion

- Differences between reflection coefficients along different azimuthal angles

$$\Delta R_{PP1} = R_{PP}^{\text{ani-visco}}(\theta, \phi_2) - R_{PP}^{\text{ani-visco}}(\theta, \phi_1)$$

$$\Delta R_{PP2} = R_{PP}^{\text{ani-visco}}(\theta, \phi_3) - R_{PP}^{\text{ani-visco}}(\theta, \phi_1)$$

$$\Delta R_{PP3} = R_{PP}^{\text{ani-visco}}(\theta, \phi_4) - R_{PP}^{\text{ani-visco}}(\theta, \phi_1)$$

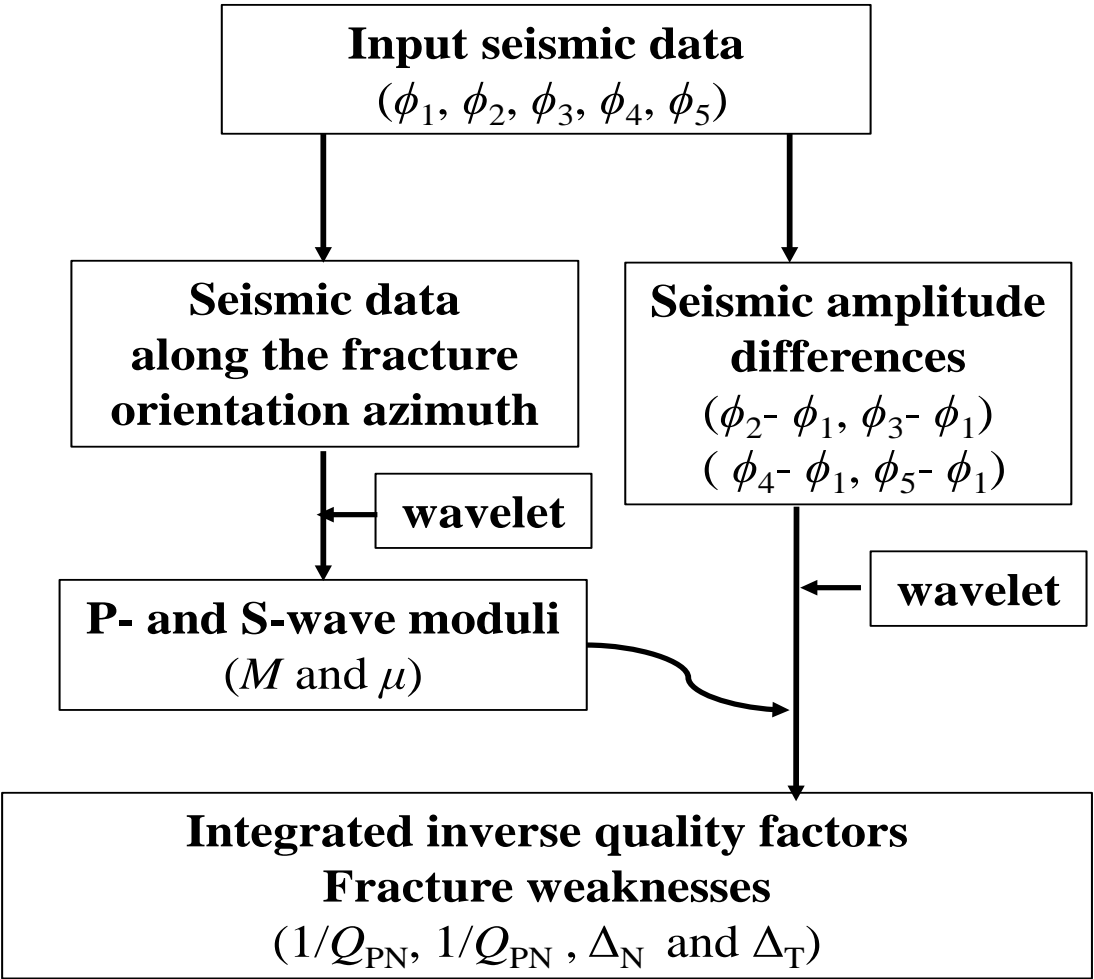
$$\Delta R_{PP4} = R_{PP}^{\text{ani-visco}}(\theta, \phi_5) - R_{PP}^{\text{ani-visco}}(\theta, \phi_1)$$

- Seismic differences

$$\Delta S_{PP} = W \Delta R_{PP}^{\text{ani-visco}}$$

- where W is seismic wavelet.

Seismic amplitude difference inversion



Workflow of seismic inversion

Seismic amplitude difference inversion

- Step1 : Utilizing seismic data along the fracture orientation azimuth to predict elastic parameters

$$\mathbf{d} = \mathbf{G}\mathbf{m}$$

- where

$$\mathbf{d} = \begin{bmatrix} \mathbf{s}(\theta_1) \\ \vdots \\ \mathbf{s}(\theta_m) \end{bmatrix}_{mn \times 1}, \mathbf{G} = \begin{bmatrix} \mathbf{WP}_M(\theta_1) & \mathbf{WP}_\mu(\theta_1) & \mathbf{WP}_\rho(\theta_1) \\ \vdots & \vdots & \vdots \\ \mathbf{WP}_M(\theta_m) & \mathbf{WP}_\mu(\theta_m) & \mathbf{WP}_\rho(\theta_m) \end{bmatrix}_{mn \times 3n}, \mathbf{m} = \begin{bmatrix} \mathbf{R}_M \\ \mathbf{R}_\mu \\ \mathbf{R}_\rho \end{bmatrix}_{3n \times 1}$$

- Solution: Least-squares

$$\mathbf{m} = \mathbf{m}_{\text{mod}} + \left(\mathbf{G}^T \mathbf{G} + \sigma^2 \right)^{-1} \mathbf{G}^T (\mathbf{d} - \mathbf{G}\mathbf{m}_{\text{mod}})$$

Seismic amplitude difference inversion

- Step2 : Using seismic differences between azimuthal data to estimate fracture weaknesses and attenuation factors

$$\mathbf{B} = \mathbf{A}\mathbf{X}$$

- where

$$\mathbf{B} = \begin{bmatrix} \mathbf{b}(\phi_2) - \mathbf{b}(\phi_1) \\ \mathbf{b}(\phi_3) - \mathbf{b}(\phi_1) \\ \mathbf{b}(\phi_4) - \mathbf{b}(\phi_1) \\ \mathbf{b}(\phi_5) - \mathbf{b}(\phi_1) \end{bmatrix}_{4mn \times 1}, \mathbf{X} = \begin{bmatrix} \mathbf{R}_{Q_{PN}} \\ \mathbf{R}_{Q_{SN}} \\ \mathbf{R}_{\Delta_N} \\ \mathbf{R}_{\Delta_T} \end{bmatrix}_{4n \times 1}$$

- Solution: An iterative approach to obtain the unknown parameter vector based on Bayesian theorem

Seismic amplitude difference inversion

- In Bayesian theorem, the posterior probability distribution function (PDF)

$$P(\mathbf{X} | \mathbf{B}) \propto P(\mathbf{B} | \mathbf{X}) P(\mathbf{X})$$

- where

Likelihood
function

$$P(\mathbf{B} | \mathbf{X}) = \frac{1}{\sqrt{2\pi\sigma_{\text{noise}}^2}} \exp\left[\frac{-(\mathbf{B} - \mathbf{A}\mathbf{X})^T (\mathbf{B} - \mathbf{A}\mathbf{X})}{2\sigma_{\text{noise}}^2}\right]$$

Gaussian
distribution

The priori
PDF

$$P(\mathbf{X}) = \frac{1}{\pi\sigma_{\mathbf{X}}} \exp\left[-\ln\left(1 + \frac{\mathbf{X}^2}{\sigma_{\mathbf{X}}^2}\right)\right]$$

Cauchy distribution

Seismic amplitude difference inversion

- In Bayesian theorem, the posterior probability distribution function (PDF)

$$P(\mathbf{X} | \mathbf{B}) = \frac{1}{\sqrt{2\pi\sigma_{\text{noise}}^2}} \frac{1}{\pi^2 \sigma_{\mathbf{X}}} \exp[-J(\mathbf{X})]$$

$$J(\mathbf{X}) = \frac{(\mathbf{B} - \mathbf{A}\mathbf{X})^T (\mathbf{B} - \mathbf{A}\mathbf{X})}{2\sigma_{\text{noise}}^2} + \ln\left(1 + \frac{\mathbf{X}^2}{\sigma_{\mathbf{X}}^2}\right)$$

- The objective function

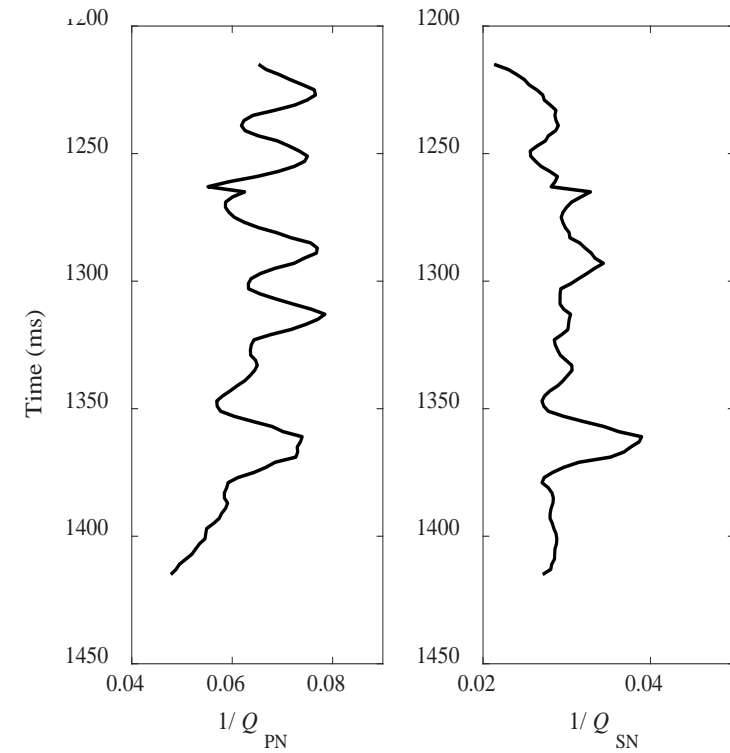
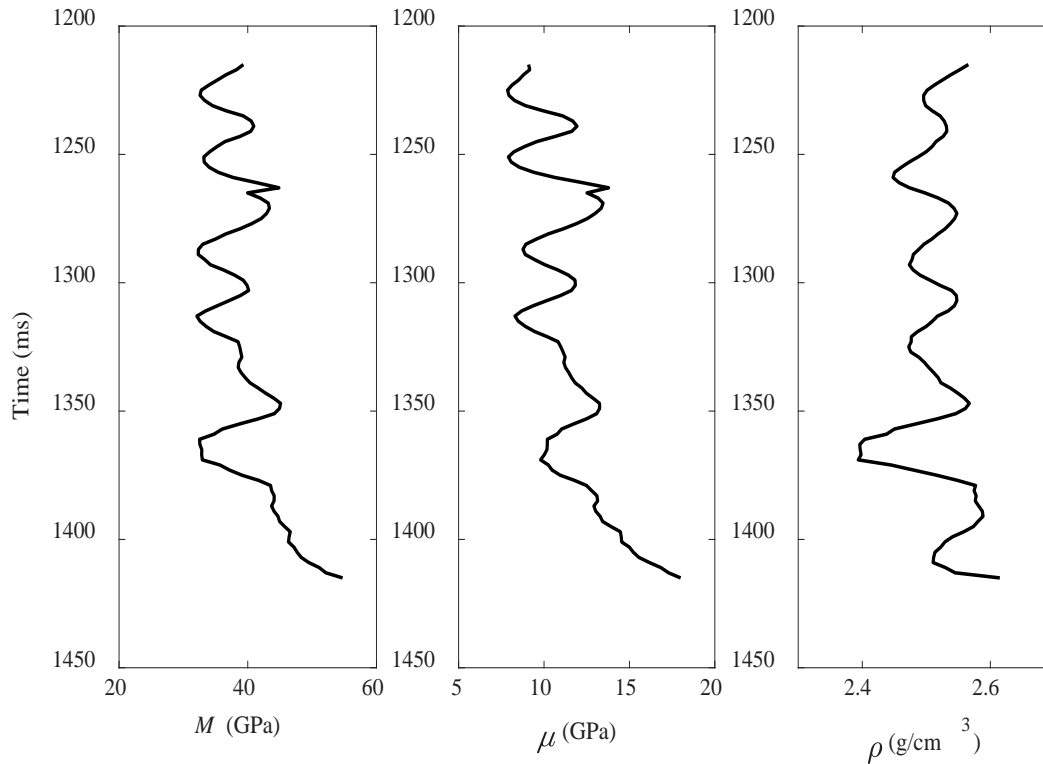
$$\frac{\partial [J(\mathbf{X})]}{\partial \mathbf{X}} = 0, \quad \left(\mathbf{A}^T \mathbf{A} + \frac{2\sigma_{\text{noise}}^2 / \sigma_{\mathbf{X}}^2}{1 + \mathbf{X}^2 / \sigma_{\mathbf{X}}^2} \right) \mathbf{X} = \mathbf{A}^T \mathbf{B}$$

- Solution of unknown parameter vector

$$\mathbf{X}_{i+1} = \mathbf{X}_i + \left(\mathbf{A}^T \mathbf{A} + \frac{2\sigma_{\text{noise}}^2 / \sigma_{\mathbf{X}}^2}{1 + \mathbf{X}_i^2 / \sigma_{\mathbf{X}_i}^2} \right)^{-1} \mathbf{A}^T (\mathbf{B} - \mathbf{A}\mathbf{X}_i)$$

Examples

- Synthetic tests

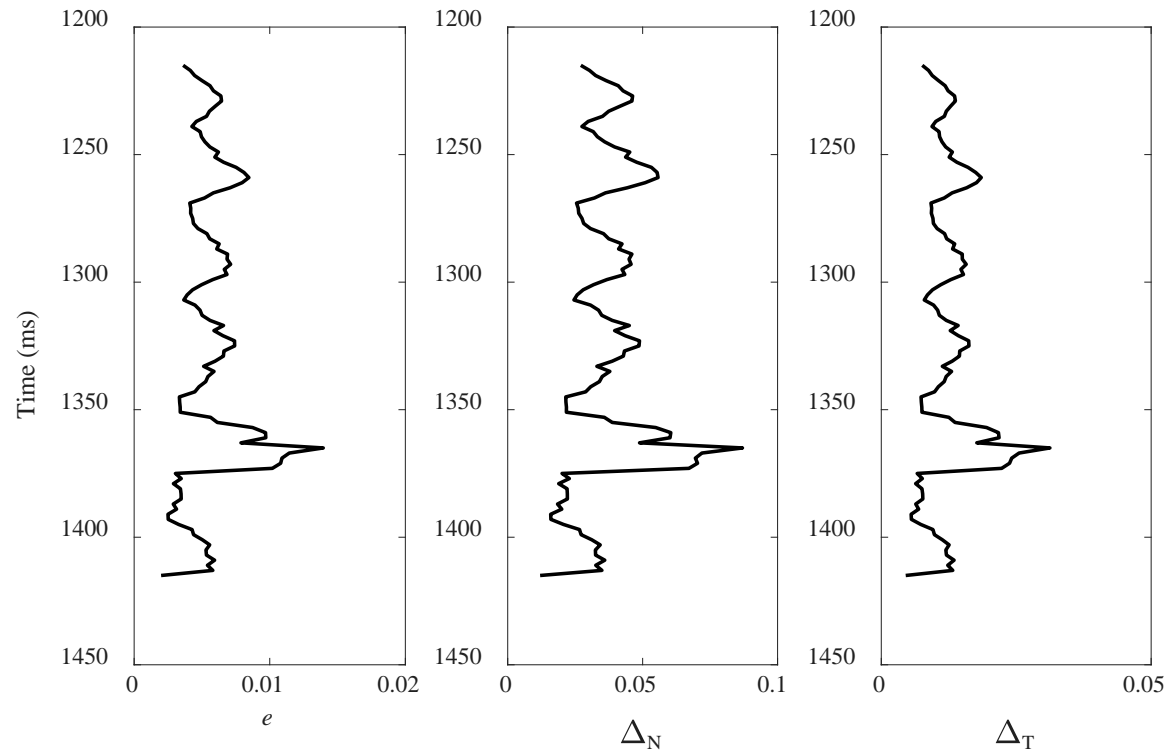


- Well log model

Calculated using empirical relationships between elastic parameters and quality factors (Mavko et al, 2009)

Examples

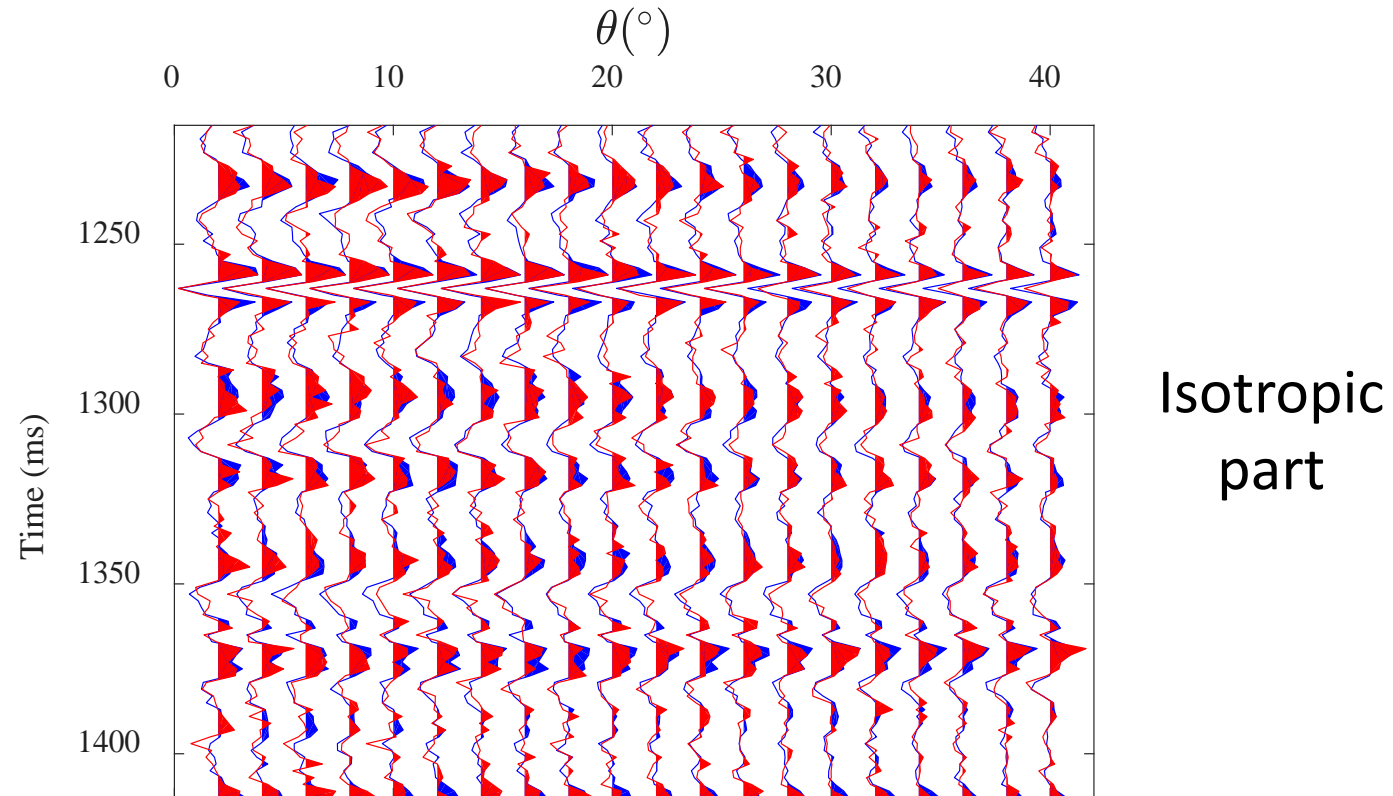
- Synthetic tests



- Well log model

Examples

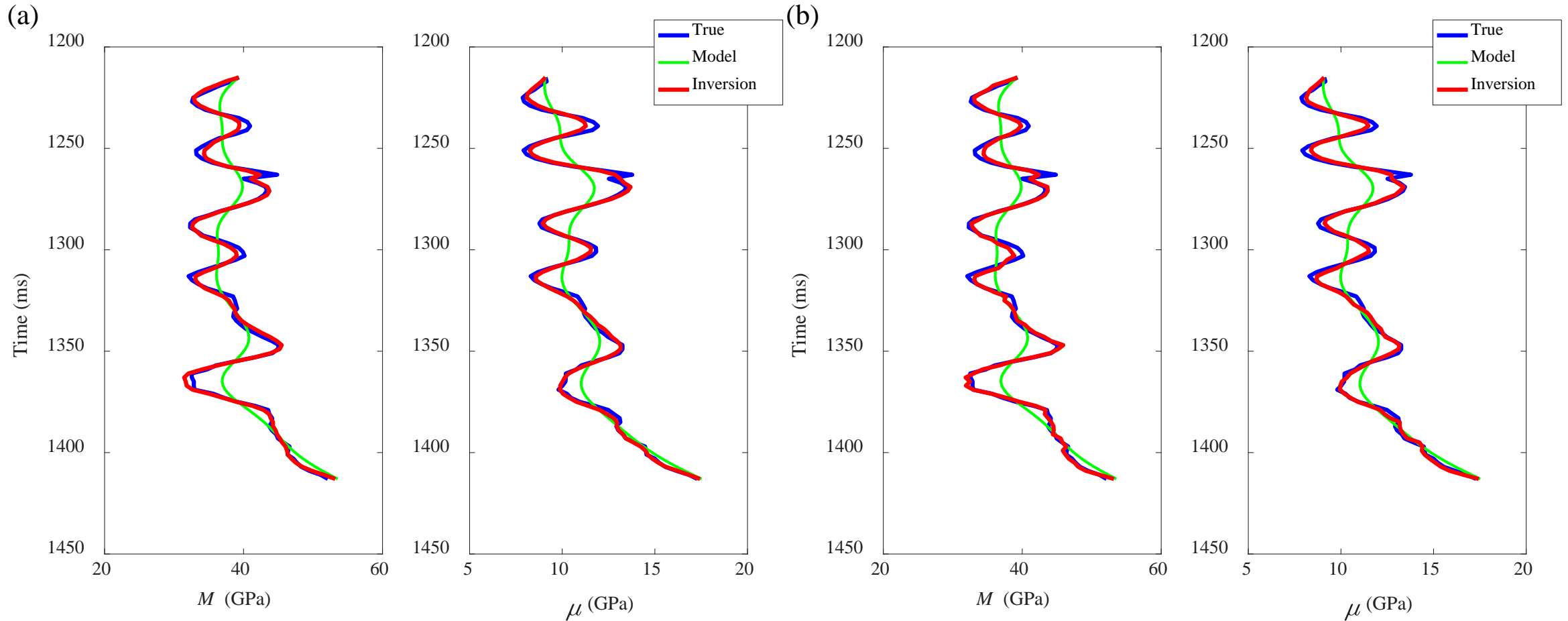
- Synthetic seismic profiles (Convolutional model)



- S/N=5(blue)
- S/N=2(red)

Examples

- Inversion results of P- and S-wave moduli

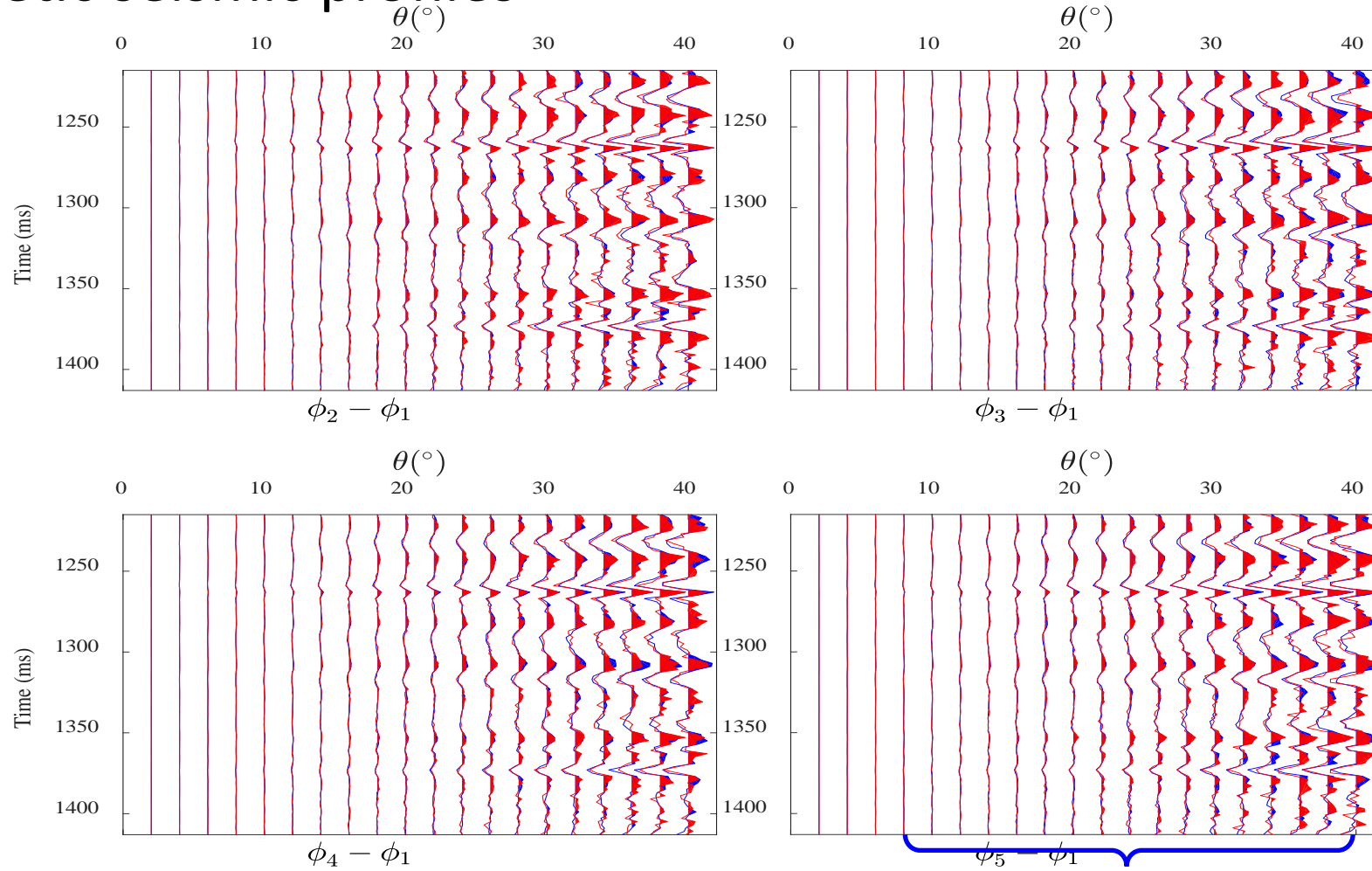


(a) S/N=5

(b) S/N=2

Examples

- Synthetic seismic profiles



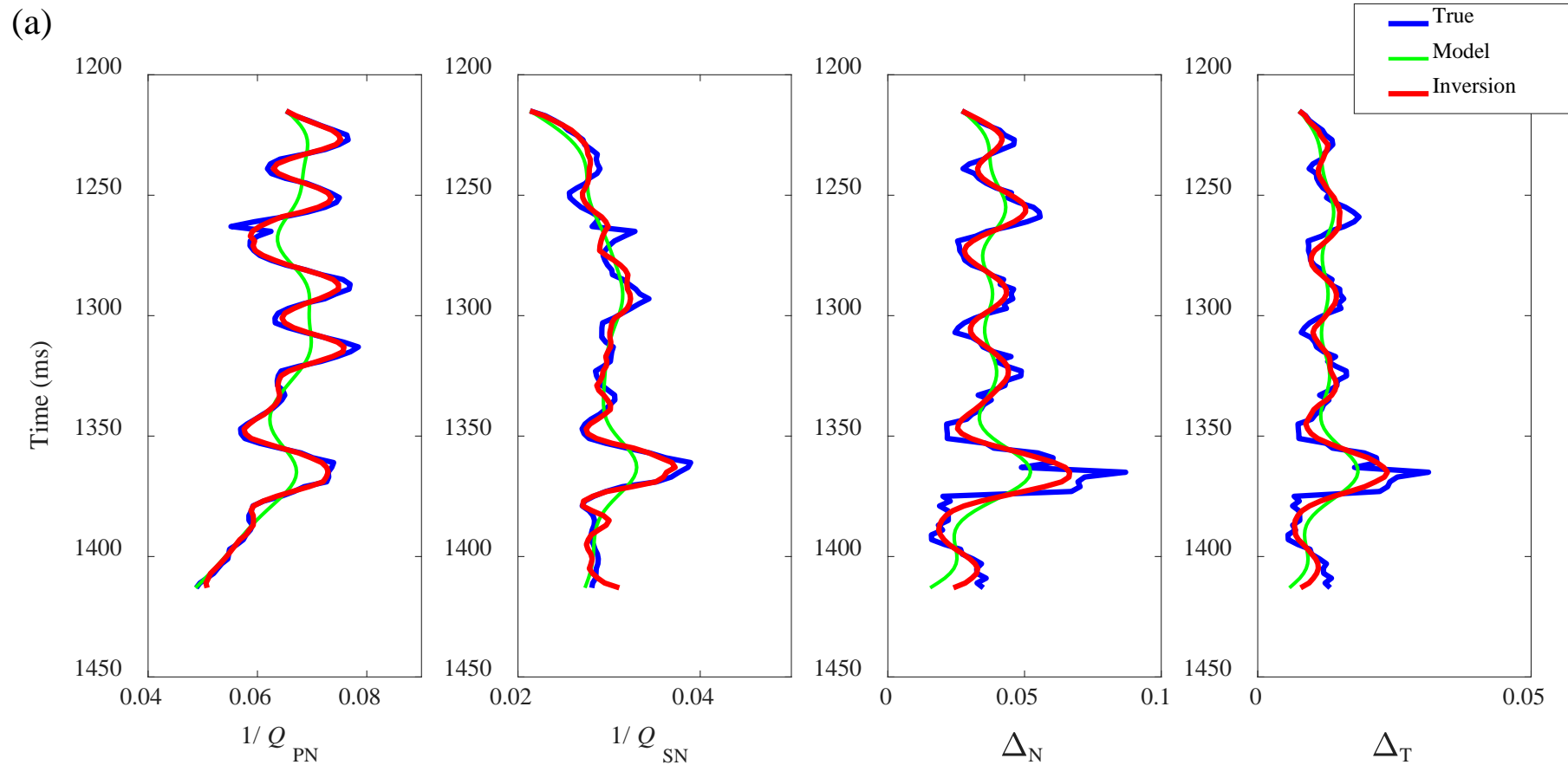
Seismic differences

- S/N=5(blue) S/N=2(red)

8-40 deg

Examples

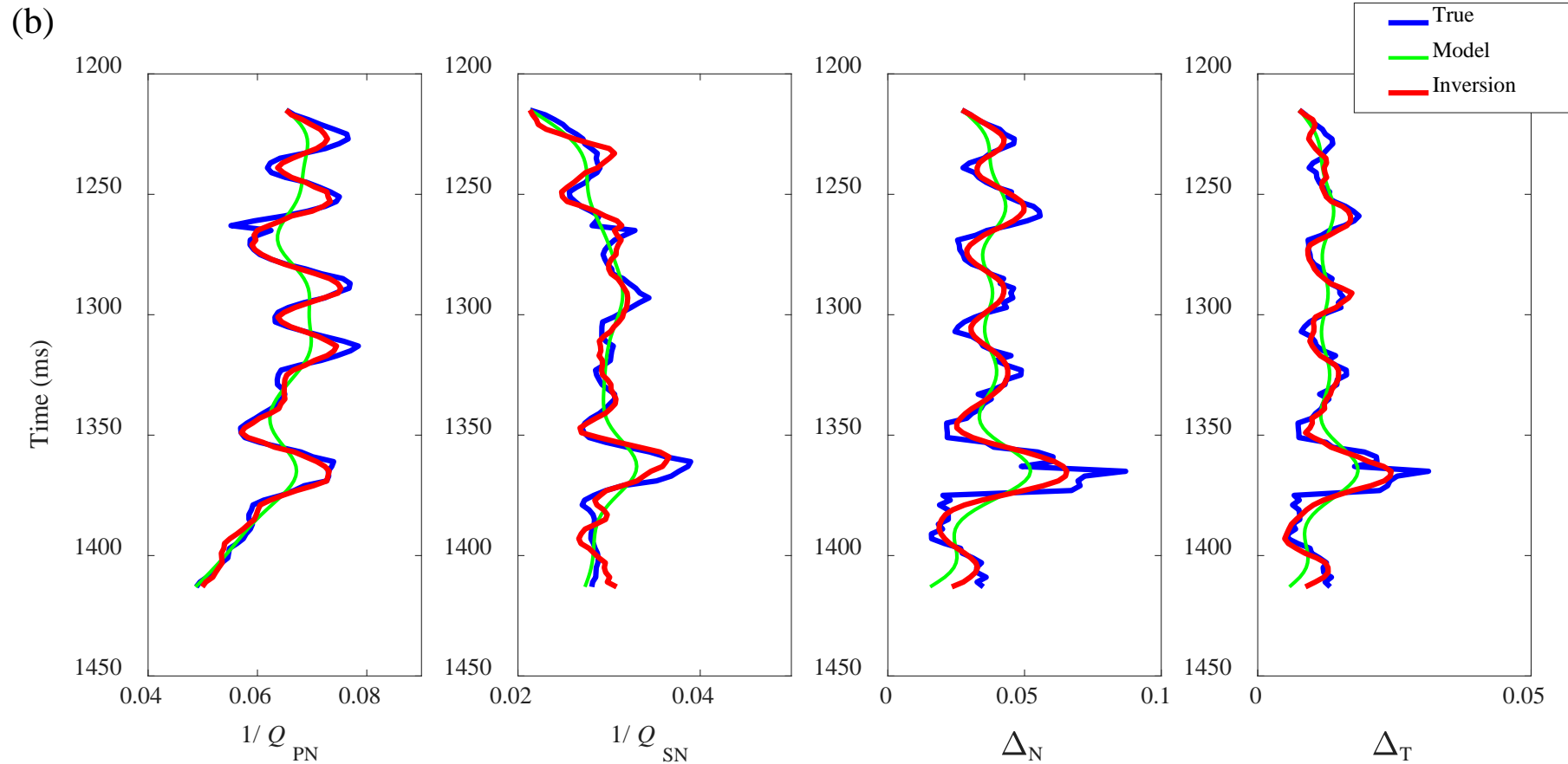
- Inversion results of fracture weaknesses and attenuation factors



(a) S/N=5

Examples

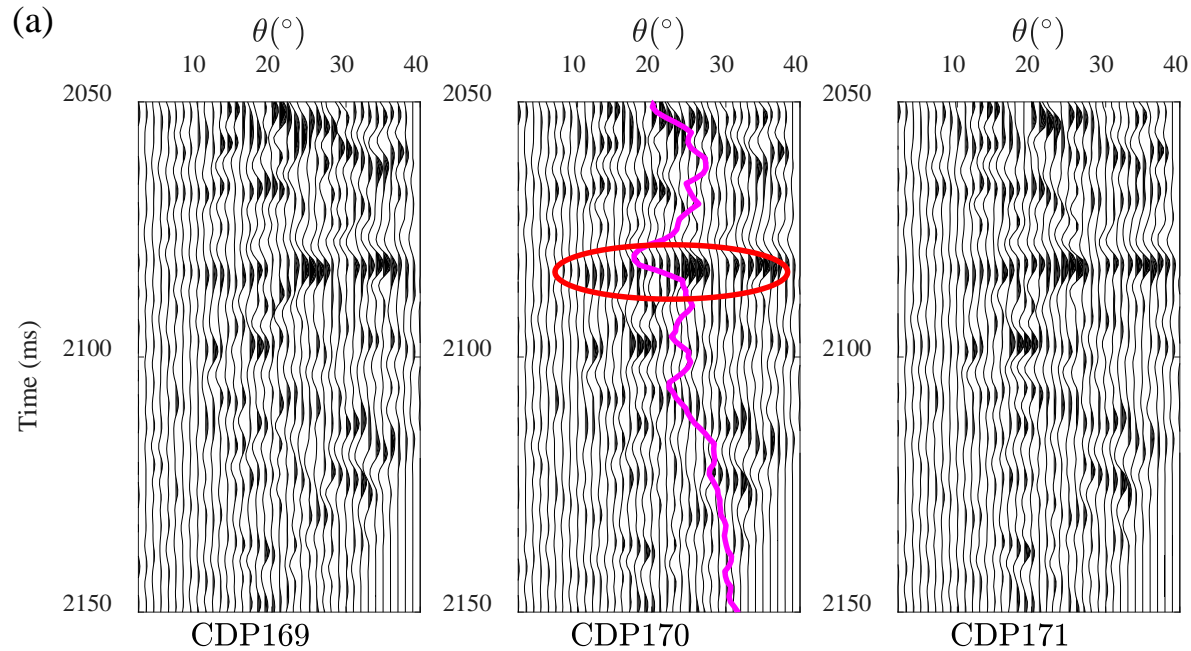
- Inversion results of fracture weaknesses and attenuation factors



(b) S/N=2

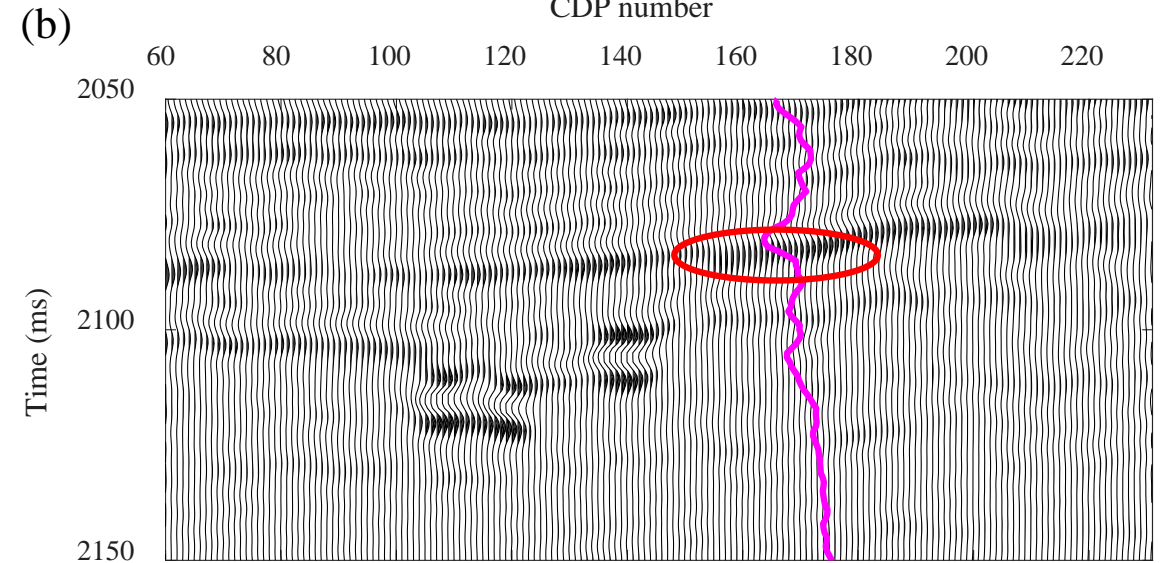
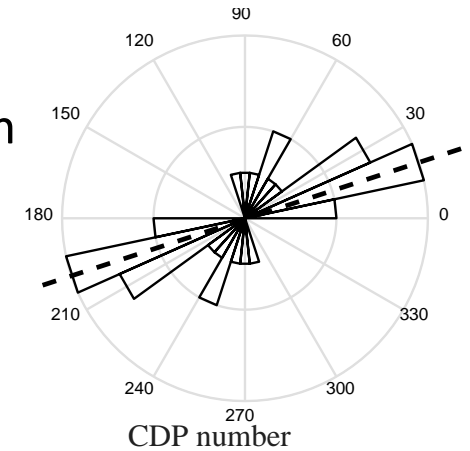
Examples

- Real data (Fractured carbonate)



(a) Angle gathers

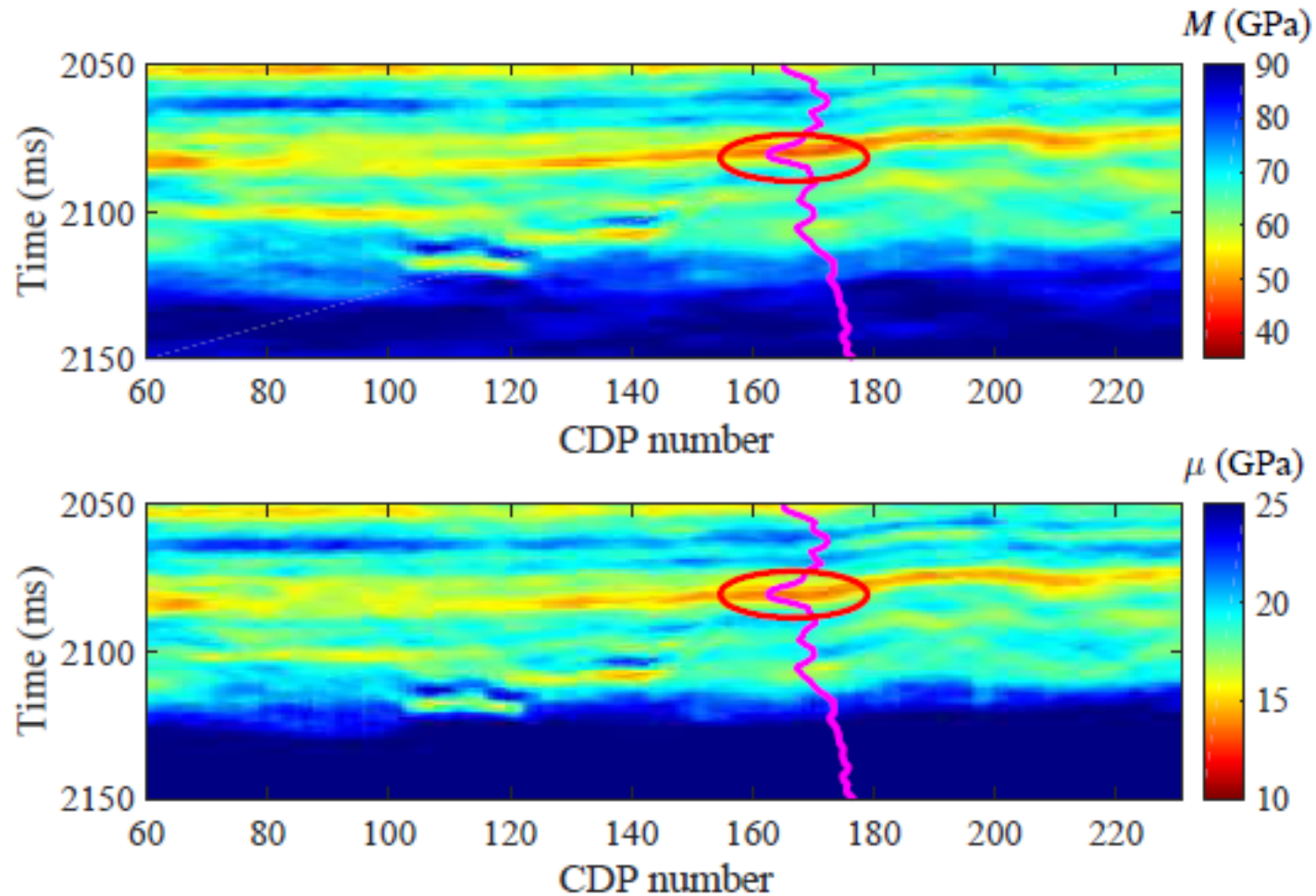
Fracture orientation



(b) Stacked seismic profile

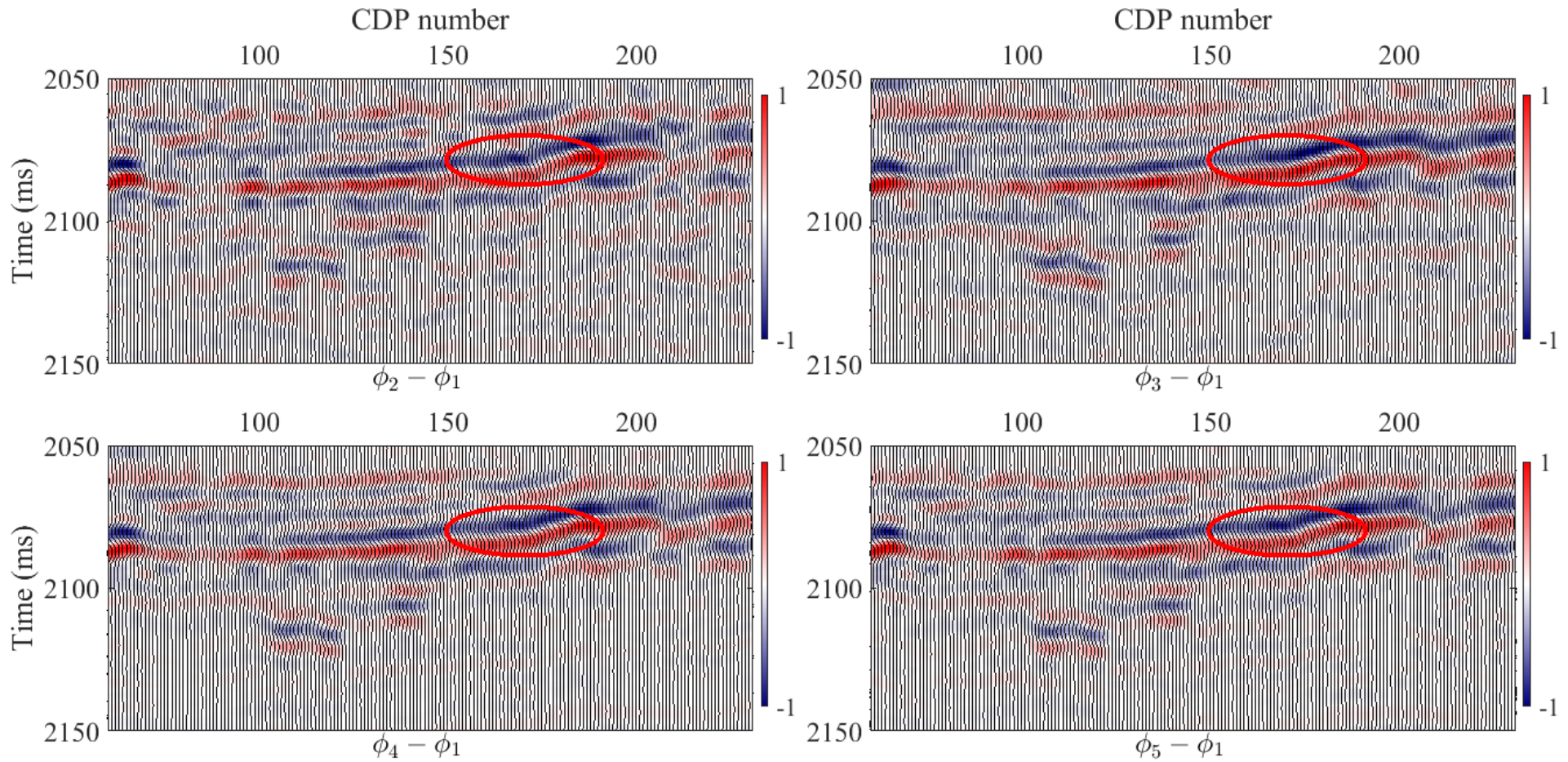
Examples

- Inversion results of P- and S-wave moduli



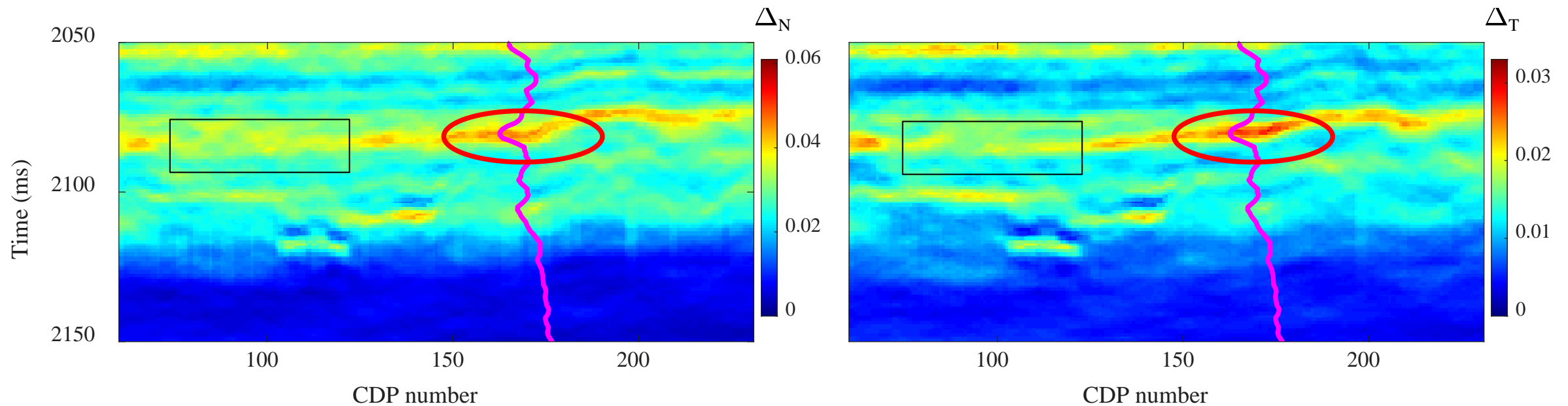
Examples

- Seismic differences



Examples

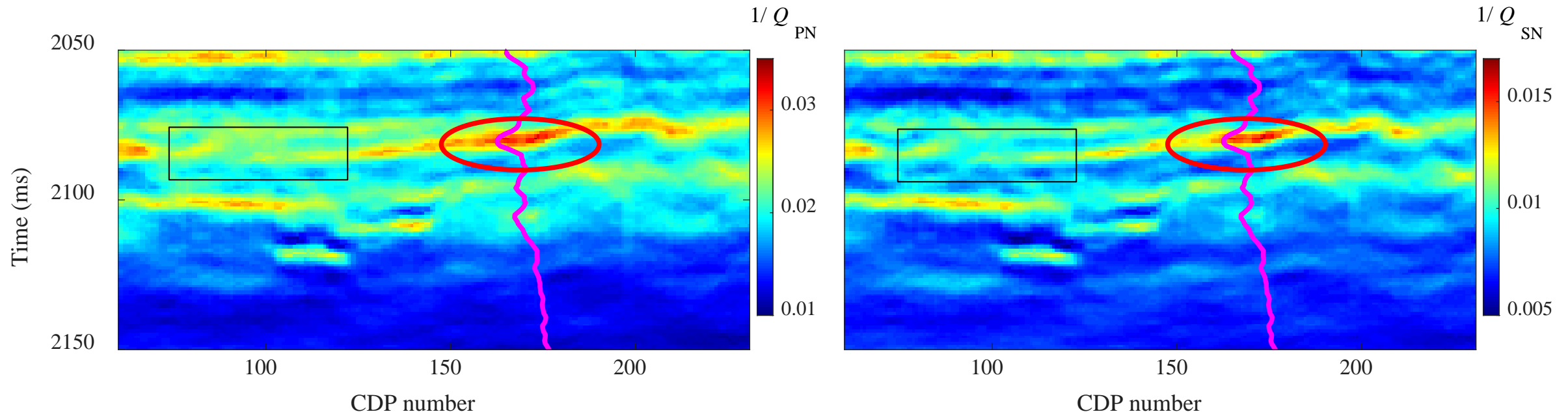
- Inversion results of fracture weaknesses and attenuation factors



There are still some locations that exhibit a high fracture weakness

Examples

- Inversion results of fracture weaknesses and attenuation factors



Detection of fractured reservoirs is improved using attenuation factors.

Discussion and Conclusions

- We have derived linearized reflection coefficient related to fracture weaknesses and attenuation factors.
- We proposed a workflow of inversion for fracture weaknesses and attenuation factors from seismic differences among azimuthal data. Tests on synthetic and real data confirm the stability and reliability of the inversion.
- Assumptions: low loss background; small fracture weaknesses; small changes in elastic properties across the interface.
- Future work: relationships among integrated, intrinsic and induced attenuation factors; combining fracture weaknesses and attenuation factors to discriminate oil bearing fractured reservoirs.

Acknowledgements

- CREWES Sponsors
- NSERC
- CFREF and Mitacs
- CREWES faculty, staff and students
- SINOPEC for data use

Thank you